

East-to-west human dispersal into Europe 1.4 million years ago

<https://doi.org/10.1038/s41586-024-07151-3>

Received: 11 July 2023

Accepted: 1 February 2024

Published online: 06 March 2024

 Check for updates

R. Garba^{1,2✉}, V. Usyk^{3,4}, L. Ylä-Mella^{5,6}, J. Kameník¹, K. Stübner⁷, J. Lachner⁷, G. Rugel⁷, F. Veselovský⁸, N. Gerasimenko⁹, A. I. R. Herries^{10,11}, J. Kučera¹, M. F. Knudsen^{12✉} & J. D. Jansen^{5✉}

Stone tools stratified in alluvium and loess at Korolevo, western Ukraine, have been studied by several research groups^{1–3} since the discovery of the site in the 1970s. Although Korolevo's importance to the European Palaeolithic is widely acknowledged, age constraints on the lowermost lithic artefacts have yet to be determined conclusively. Here, using two methods of burial dating with cosmogenic nuclides^{4,5}, we report ages of 1.42 ± 0.10 million years and 1.42 ± 0.28 million years for the sedimentary unit that contains Mode-1-type lithic artefacts. Korolevo represents, to our knowledge, the earliest securely dated hominin presence in Europe, and bridges the spatial and temporal gap between the Caucasus (around 1.85–1.78 million years ago)⁶ and southwestern Europe (around 1.2–1.1 million years ago)^{7,8}. Our findings advance the hypothesis that Europe was colonized from the east, and our analysis of habitat suitability⁹ suggests that early hominins exploited warm interglacial periods to disperse into higher latitudes and relatively continental sites—such as Korolevo—well before the Middle Pleistocene Transition.

Knowledge of early human dispersal patterns is founded on the identification of fossils and lithic artefacts backed by absolute dating^{10–12}. When considering Europe's first hominins, several archaeological sites are accepted as predating the Matuyama–Brunhes geomagnetic polarity reversal (around 0.77 Ma) and some are claimed to predate the Jaramillo subchron (around 1.07–0.99 Ma)^{7,8,12,13}, although these claims have been challenged^{11,14}. The current situation is that securely dated sites are few, and any assessment of the first human dispersals into Europe hinges on the choice of bona fide chronologies.

To the east of Europe stands the key site of Dmanisi, Georgia (Fig. 1a), where layers containing hominin cranial remains^{6,15,16} and stone tools are dated securely to around 1.85–1.78 Ma (ref. 6). A trail from Africa to Dmanisi via the Levantine corridor accords with the Mode-1 (Oldowan) lithic artefacts documented in Jordan's Zarqa Valley, as early as around 2.5 Ma (ref. 17). The earliest precisely dated evidence of humans in Europe occurs at two southwestern sites (Fig. 1a): Atapuerca, Spain, where the oldest human fossils at Sima del Elefante are reported at around 1.2–1.1 Ma (ref. 7); and Vallonnet Cave, southern France, where lithic artefacts are constrained to around 1.2–1.1 Ma (ref. 8). However, the vast spatial and temporal gap that separates the Caucasus and southwestern Europe leaves key aspects of the first human dispersal into Europe largely unresolved^{7,11,12,14}. An eastern route via Asia Minor (Fig. 1a) is hinted at by a skull fragment in Kocabaş, Turkey, dated to at least 1.1 Ma (ref. 18)—notwithstanding the dating complications at that site (Supplementary Information). Indeed, a major obstacle to testing models of human dispersal is the dating deficiencies that beset most Palaeolithic sites^{10,14}. Here we apply burial dating with

cosmogenic nuclides, beryllium-10 (¹⁰Be) and aluminium-26 (²⁶Al), to the lowermost cultural layer at Korolevo, western Ukraine (Figs. 1 and 2). Located midway between the Caucasus and southwestern Europe, Korolevo is held to be among the northernmost (48.2° N) Early Palaeolithic sites globally. We also examine the potential habitat suitability⁹ of the Early Pleistocene Korolevo in light of orbital-scale climatic variability.

The Korolevo site, western Ukraine

Korolevo lies close to where the Tysa River (a tributary of the Danube) leaves the eastern Carpathian Mountains and spreads southwestward across the Pannonian Plain (Fig. 1a). The multi-level, open-air archaeological site is located in an andesite quarry in which an accumulation of alluvium and loess is preserved in a river terrace between two low bedrock hills, Gostry Verkh (Fig. 1b) and Beyvar (Supplementary Information). Since its discovery by V. N. Gladilin in 1974, numerous archaeological^{1–3,19,20}, palaeoecological^{1,19,21,22} and chronometric^{21–23} studies have been conducted. This previous work has established Korolevo as a key site^{3,14,24,25} of early hominin occupation north of the Alps.

The reference stratigraphic profile at Gostry Verkh (Fig. 1b), known as Korolevo I^{19,21}, comprises a relatively simple stack of sub-horizontal fluvial gravels and sands topped by successive loess–palaeosol units, including several erosional breaks (Fig. 2). The existing chronology at Korolevo I is based on magnetostratigraphy^{2,19,21–23} and thermoluminescence dating of unheated quartz^{1,22}. Pollen analyses^{1,21} within the stratigraphic profile at Korolevo I indicate fluctuating cooler and

¹Nuclear Physics Institute, Czech Academy of Sciences, Řež, Czechia. ²Institute of Archaeology Prague, Czech Academy of Sciences, Prague, Czechia. ³Institute of Archaeology, National Academy of Sciences of Ukraine, Kyiv, Ukraine. ⁴Institute of Archaeology Brno, Czech Academy of Sciences, Brno, Czechia. ⁵GFU Institute of Geophysics, Czech Academy of Sciences, Prague, Czechia. ⁶Department of Physical Geography and Geoecology, Charles University, Prague, Czechia. ⁷Institute of Ion Beam Physics and Materials Research, Helmholtz-Zentrum Dresden-Rossendorf, Dresden, Germany. ⁸Czech Geological Survey, Prague, Czechia. ⁹Taras Shevchenko National University of Kyiv, Kyiv, Ukraine. ¹⁰Department of Archaeology and History, La Trobe University, Melbourne, Victoria, Australia. ¹¹Palaeo-Research Institute, University of Johannesburg, Johannesburg, South Africa. ¹²Department of Geoscience, Aarhus University, Aarhus, Denmark. ✉e-mail: garba@ujf.cas.cz; mfk@geo.au.dk; jdj@ig.cas.cz

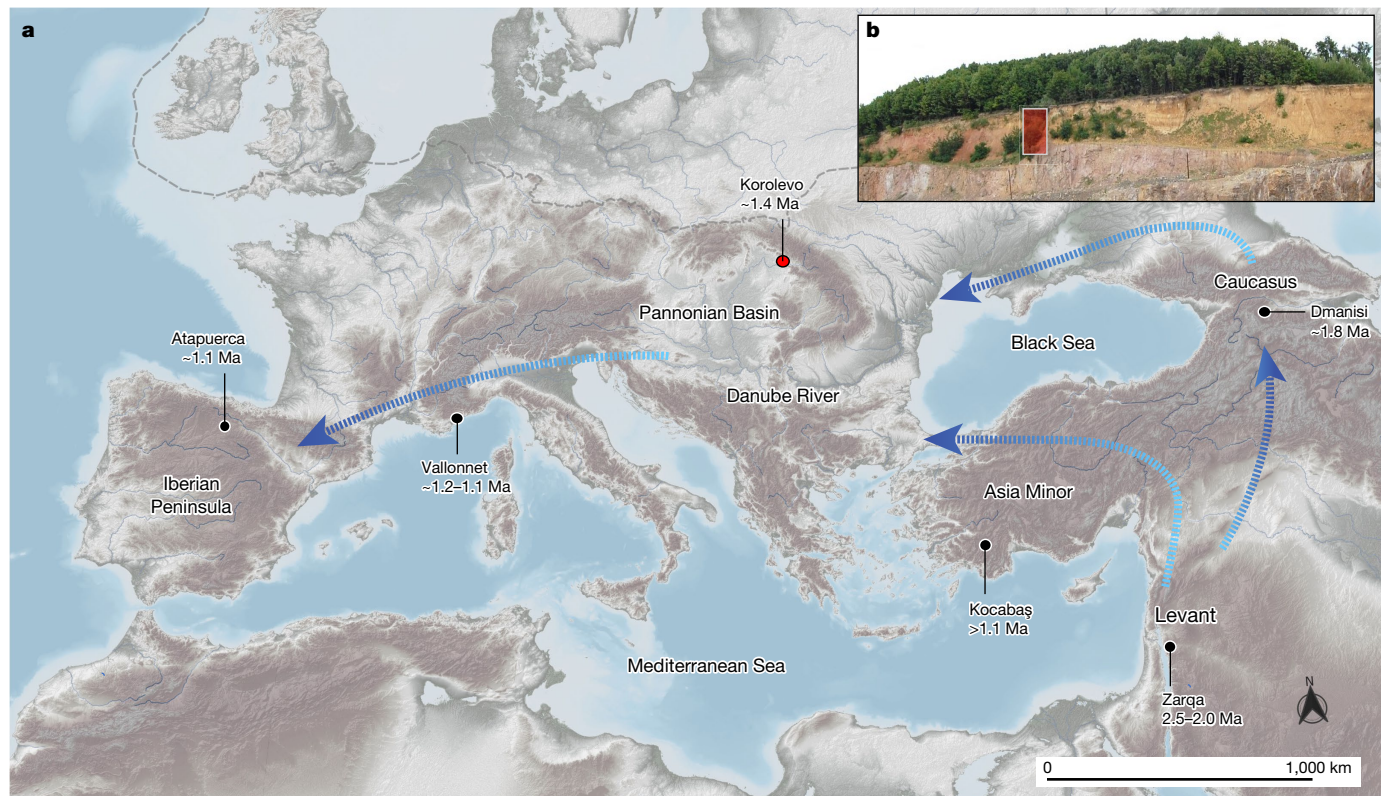


Fig. 1 | First peopling of Europe. **a**, Archaeological sites and dispersal routes noted in the text. The maximum extent of the Eurasian ice sheets⁴⁵ is indicated with grey dashes. Blue arrows indicate possible early human dispersal routes.

Base map data source: the GEBCO 2022 Grid (<http://gebco.net>), generated using QGIS v.3.26 (EPSG:3035). **b**, Korolevo I, Gostry Verkh, viewed from the Beyvar hill with excavation XIII (red box).

warmer conditions that may represent orbital-scale climate cycles (Supplementary Information).

The Matuyama–Brunhes geomagnetic reversal (around 0.77 Ma)¹³ was first identified below cultural level VI (refs. 2,23) and later confirmed by a second study²¹ (Fig. 2). A third magnetostratigraphic analysis²² (Supplementary Information) corroborated the location of the Matuyama–Brunhes boundary and indicated the presence of inclination–declination variability and normal geomagnetic polarity near the base of the Gostry Verkh profile (Fig. 2), which was tentatively ascribed to the Jaramillo subchron (1.07–0.99 Ma)¹³. Thermoluminescence dating by two research groups^{1,22} yielded conflicting ages, but the absence of any laboratory documentation precludes an objective assessment (Supplementary Information). Although the age of the lowermost lithic assemblage (level VII) remains poorly constrained, three erosional hiatuses between the Matuyama–Brunhes boundary and level VII (Fig. 2) suggest an age considerably beyond 0.77 million years.

Lithic artefacts

The archaeological sequence of cultural layers at Korolevo I contains evidence of repeated hominin occupation over several hundred thousand years, although no fossils have been found. Following a previous study³, the sequence is subdivided into seven cultural layers spanning the Early Palaeolithic to the Early Upper Palaeolithic. More than 95% of the lithic artefacts recorded at Korolevo are composed of hyalodacite, a microcrystalline volcanic rock outcropping in the Beyvar hill, the knappable properties of which²⁶ might account for the multi-period occupation at this site.

The Early Palaeolithic lithic artefacts occur in two assemblages, levels VII and VI³. Level VII (excavation XIII, Fig. 2) yielded a total of 33 lithic artefacts, including chunks, flakes, cores and polyhedrons^{2,3}. Of these, two tools—a chopper core, and a flake with bifacial treatment

(Fig. 3)—were identified, both reflecting hard hammer reduction. Although they lie within an alluvial channel deposit, we detected no damage or polish associated with fluvial transport. These 33 artefacts from level VII are a subset of a larger set of 1,800 artefacts from nearby Beyvar²⁰, including cores, tools and flakes also assigned to level VII on the basis of weathering attributes. However, this collection is poorly constrained stratigraphically (Supplementary Information).

A younger Early Palaeolithic assemblage, level VI (Fig. 2), yielded more than 5,000 artefacts of a flake-based industry represented by a simple unidirectional, parallel and rare centripetal reduction strategy^{2,3}. The assemblage is characterized by a few choppers, an absence of hand axes or cleavers and a diversity of side scrapers, sometimes with bifacial treatment. The Middle Palaeolithic assemblages (Fig. 2: levels Va, V, III, IIb, IIa and II) belong to a range of industries, including Micoquian, Levallois and Early Middle Palaeolithic industries with bifacial blade points². The youngest assemblage, level Ia, consists of an Early Upper Palaeolithic industry that comprises a blade-based industry of non-Aurignacian typology².

Results of burial dating

The ²⁶Al–¹⁰Be cosmogenic nuclide inventory of seven gravel clasts from the lowermost cultural layer (level VII) was measured²⁷ to constrain the age of the first hominin presence at Korolevo using P-PINI (particle-pathway inversion of nuclide inventories)^{5,28} and isochron^{4,29,30} burial-dating methods. The seven clast samples yielded high and relatively uniform ¹⁰Be concentrations (1.0×10^6 – 1.7×10^6 at g^{-1}) and low ²⁶Al/¹⁰Be ratios of 3.0 to 3.5 (Table 1, Methods and Supplementary Information). This combination of abundant ¹⁰Be and low ²⁶Al/¹⁰Be ratios is ideal for burial dating; it indicates that the clasts were exposed at the surface for sufficient time to accumulate a large inventory of ¹⁰Be and ²⁶Al before their lengthy burial. The seven clast samples cluster

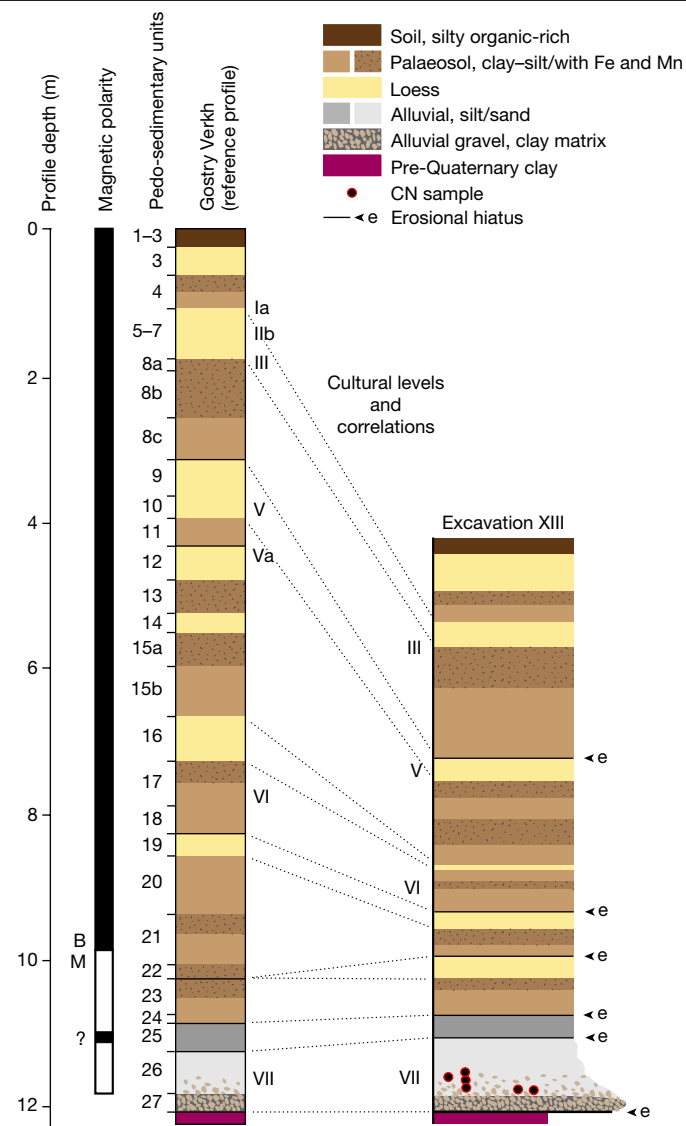


Fig. 2 | Composite stratigraphic section at Korolevo I. Excavation XIII (refs. 1,3) (right) and the Gostry Verkh reference profile (left), with magnetic polarity^{21–23} and cultural levels^{1,3,21} (I to VII) containing lithic artefacts^{2,3}. The 27 pedo-sedimentary units defined in a previous study²¹ represent the most comprehensive stratigraphic work conducted at the site. Below the Matuyama–Brunhes boundary (B and M letters), a short interval of normal geomagnetic polarity potentially represents either the Jaramillo subchron (1.07–0.99 Ma) or the Cobb Mountain subchron (1.22–1.18 Ma). Mode-1 lithic artefacts are contained within level VII, which was sampled for cosmogenic nuclide (CN) burial dating.

tightly around the isochron (Fig. 4b), which suggests that none of the clasts were reworked from older deposits. The tight concentration of data points along the isochron (mean square weighted deviation (MSWD) = 0.84) strongly suggests that all samples experienced a simple two-stage burial history that included one period of exposure followed by one period of burial; it is very unlikely that a more complex burial history would result in such low dispersion.

We obtain an isochron burial age of 1.42 ± 0.28 Ma ($\pm 1\sigma$) for cultural level VII at Korolevo I (Supplementary Information). The large (20%) uncertainty range is the product of the high ^{10}Be concentration (more than 1.0×10^6 at g^{-1}) in all seven samples, which limits the spread of the data and results in a large uncertainty at the intercept (Fig. 4b), representing post-burial production. The age can be better constrained by considering physically plausible estimates of post-burial production in

a forward model such as P-PINI. Application of the P-PINI method to the same seven samples yields a burial age of 1.42 ± 0.10 Ma ($\pm 1\sigma$) (Fig. 4). Applying the P-PINI model to ^{10}Be – ^{26}Al data reported from Sima del Elefante⁷ yields a burial age of 1.12 ± 0.16 Ma ($\pm 1\sigma$) for the fossil-bearing unit TE9 using a Bayesian approach applied to samples C-TE9b and C-TE7 (Methods).

Earliest hominin presence in Europe

We set out to determine the burial age of the lowermost cultural layer (level VII) at Korolevo I, using two well-tested approaches to cosmogenic nuclide burial dating. The resulting ages ($\pm 1\sigma$) are 1.42 ± 0.28 Ma and 1.42 ± 0.10 Ma using the isochron burial method and P-PINI, respectively. Although the methods yield overlapping ages, we favour the P-PINI result for the Korolevo setting because it readily accounts for (1) non-steady erosion in the catchment before sediment burial; (2) catchments with elevation-dependent $^{26}\text{Al}/^{10}\text{Be}$ ratios; (3) sample-specific source elevations; and (4) the slow accumulation of loess units in the profile over time (Fig. 2). Moreover, P-PINI delivers a tighter uncertainty range because the intercept and post-burial production are constrained by the forward model.

The burial age of cultural level VII is consistent with the previous magnetostratigraphy²², which identified the Matuyama–Brunhes boundary (around 0.77 Ma) at 1.39 m above level VII in the Gostry Verkh profile, along with a tentative suggestion of the Jaramillo subchron near the base (Fig. 2). This hint of normal geomagnetic polarity could represent either the Jaramillo subchron (1.07–0.99 Ma) or the Cobb Mountain subchron (1.22–1.18 Ma)¹³. In any case, the magnetostratigraphy is compatible with our cosmogenic nuclide burial age because an erosional hiatus occurs between level VII and the Jaramillo or Cobb Mountain signal (Fig. 2 and Supplementary Information). Although the characteristic fragmentation of terrestrial stratigraphy presents a common difficulty for geomagnetic chronometry, such limitations do not affect our burial dating. A well-founded strength of the open-air Korolevo I profile is its relatively simple layer-cake stratigraphy, comprising alluvial sediments topped by successive loess–palaeosol units (Fig. 2). None of the confounding factors that can beset caves, such as complex stratigraphy or major post-depositional disturbances^{7,8,18,30}, occur at Korolevo.

The P-PINI burial age (1.42 ± 0.10 Ma) demonstrates unequivocally that Korolevo I (level VII) predates both the Jaramillo subchron (at 95% confidence level) and the Middle Pleistocene Transition (around 1.2–0.8 Ma)³¹, and thereby rules out the hypothesis of a human migration ‘bottleneck’^{11,14} into Europe before or during the Jaramillo subchron (1.07–0.99 Ma). Considering our recalculated age of 1.12 ± 0.16 Ma for the hominin fossil-bearing unit, TE9, at Sima del Elefante⁷, and the 1.2–1.1 Ma occupation of Vallonnet Cave⁸, Korolevo is now established as the earliest securely dated hominin presence in Europe. The absence of fossils precludes certitude, but the timing suggests that *Homo erectus* resided in this area of present-day western Ukraine well before the Middle Pleistocene Transition.

The Danube dispersal route into Europe

Korolevo bridges the spatial and temporal gap in terms of human dispersal between the Caucasus (around 1.85–1.78 Ma at Dmanisi)^{6,16} and southwestern Europe (around 1.2–1.1 Ma at Atapuerca⁷ and Vallonnet⁸), and the relationships among lithic assemblages have the potential to reveal the spread of cultural traits associated with human migration. The Korolevo I (level VII) lithic assemblage is characteristic of a Lower Palaeolithic industry (without hand axes) defined as the Mode-1 core-and-flake industry first documented in East Africa³². The lithic assemblage reported from the Zarqa Valley, Jordan¹⁷, which comprises a simple tool kit of choppers showing unidirectional and parallel reduction, is highly compatible with Korolevo’s level VII. The lithic assemblage

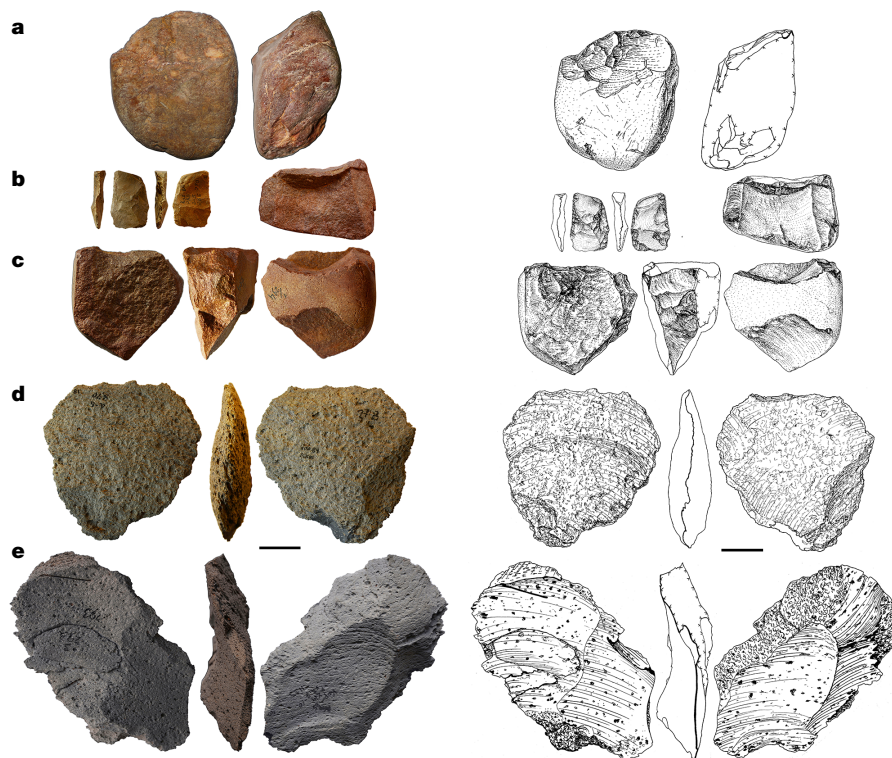


Fig. 3 | Selected lithic artefacts from Korolevo I, level VII. a, Chopper core. **b,** Flake with bifacial treatment. **c,** Multi-platform core. **d,** Kombewa flake. **e,** Flake with parallel scar pattern. Additional artefacts are presented in Supplementary Fig. 3. Scale bars, 3 cm. The drawings in a–c are modified from ref. 3.

reported from Dmanisi^{15,33} also shows important similarities, such as the simple unidirectional (unipolar) and parallel reduction strategy, and the presence of chopper cores and polyhedrons, although Korolevo lacks advanced side scrapers. The presence of bipolar reduction in assemblages from early (>1 Ma) Iberian sites suggests a more distant relationship^{34–36}, along with differing modes of resource exploitation. However, the limited lithic material reported from both Atapuerca⁷ and Vallonnet⁸ precludes detailed comparison with Korolevo I.

Our findings at Korolevo provide the first primary evidence advancing the hypothesis that Europe was colonized from the east^{7,12}. A plausible dispersal scenario is that the Korolevo hominins stem from the Levant via Asia Minor, the Danube corridor and the Pannonian Basin^{12,14,37,38} (Fig. 1). Alternatively, a route from the Caucasus and to the north of the Black Sea remains a possibility. We recognize that hominin

dispersal surely did not unfold as a unidirectional march from A to B, but additional securely dated sites are needed to build upon our simple sketch. Moreover, other early hominin sites^{34,36,39–43} could change the picture of Europe’s colonization once robust chronologies become available. But for now, we can say that Korolevo’s occupation at around 1.4 Ma directly challenges the proposal⁸ that people moved to higher latitudes only after the widespread colonization of southern Europe by around 1.2 Ma.

Northern limits of habitat suitability?

Located at 48.2° N, Korolevo is the northernmost known presence of (we assume) *H. erectus*. These early humans are already regarded as flexible generalists^{9,44}, but their presence at this latitude and in such a continental setting provokes some rethinking. We note that there is a low likelihood of finding early European hominin sites even farther north—not because they did not exist, but because the Fennoscandian Ice Sheet extended as far south as the Carpathians on at least two occasions in the last half a million years⁴⁵ (Fig. 1). Early hominin sites farther north are likely either to be destroyed or to lie deeply buried.

Clues about where and when conditions were ripe for colonization are offered by a palaeoclimate modelling analysis that evaluates hominin habitat suitability on a global scale over the past two million years⁹. Earth’s orbital-scale climate cyclicity shifted from 41,000 to 100,000 years during the Middle Pleistocene Transition (1.2–0.8 Ma)³¹, meaning that *H. erectus* occupied Korolevo at a time of relatively short glacial–interglacial cycles. The timing at Korolevo (1.42 ± 0.10 Ma) coincides with three interglacial warm periods defined by marine isotope stages (MIS) 47, 45 and 43 (Fig. 4a), and pollen analyses within the level VII sediments^{1,21} indicate warm conditions (Supplementary Information). These interglacials apparently offered some of the most favourable conditions for *H. erectus* during the half million years before the Middle Pleistocene Transition. MIS 47, 45 and 43 were among the warmest interglacials of the Early Pleistocene, and all show high habitat

Table 1 | Accelerator mass spectrometry analysis of ¹⁰Be and ²⁶Al concentrations

CN sample	¹⁰ Be [¹⁰ Be at g ⁻¹] ^a	¹⁰ Be uncert. [10 ⁶ at g ⁻¹]	²⁶ Al [¹⁰ Be at g ⁻¹] ^b	²⁶ Al uncert. [10 ⁶ at g ⁻¹]	²⁶ Al/ ¹⁰ Be	²⁶ Al/ ¹⁰ Be uncert.
KOR-ISO-01	1.634	0.033	4.92	0.19	3.01	0.13
KOR-ISO-03	1.653	0.033	5.26	0.20	3.18	0.14
KOR-ISO-04	1.024	0.022	3.48	0.17	3.41	0.18
KOR-ISO-05	1.284	0.027	4.45	0.24	3.48	0.20
KOR-ISO-07A	1.504	0.034	4.57	0.23	3.05	0.17
KOR-ISO-08	1.698	0.034	5.45	0.24	3.21	0.16
KOR-ISO-09	1.154	0.024	4.06	0.19	3.53	0.18

^aAssumed ¹⁰Be half-life of 1.387 million years (refs. 46,47).

^bAssumed ²⁶Al half-life of 0.705 million years (ref. 48).

All uncertainties (uncert.) ±1σ. See Supplementary Information for extended cosmogenic nuclide data. The secondary standards SMD-Be-12 (ref. 49) and SMD-Al-11 (ref. 50) were used for normalization of measured ¹⁰Be/^{Be} and ²⁶Al/^{Al} ratios, respectively.

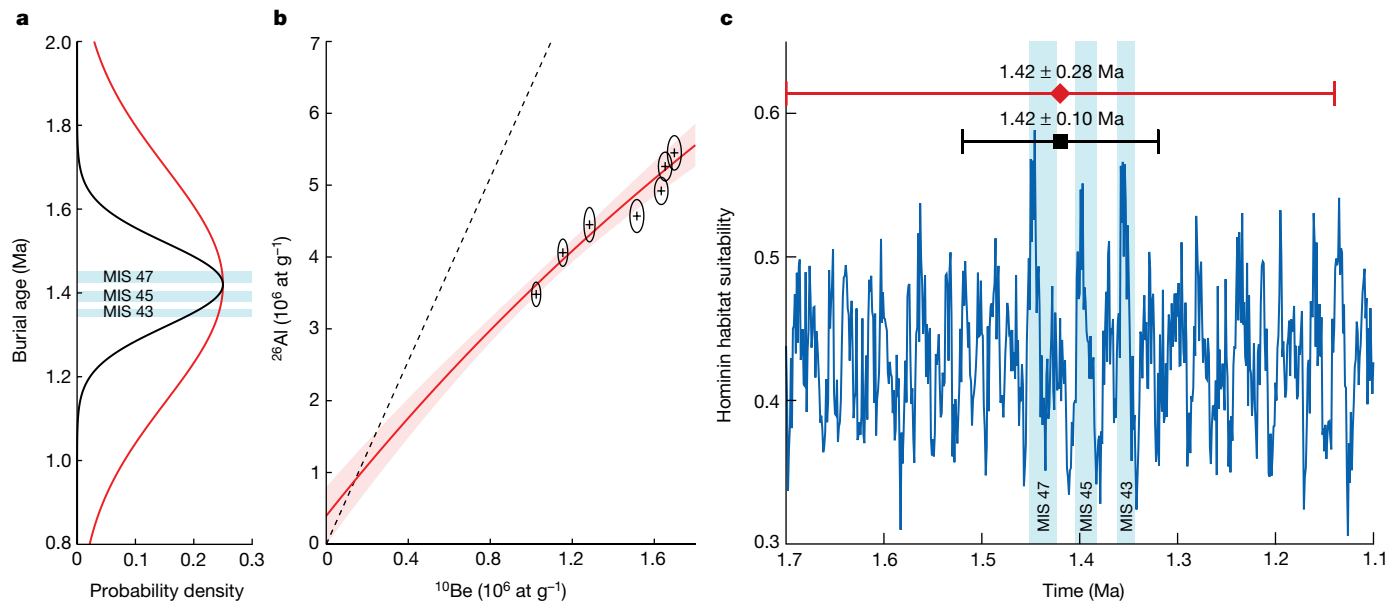


Fig. 4 | Cosmogenic nuclide burial ages for Korolevo I, level VII. a, Main probability plot for the P-PINI (black curve; 1.42 ± 0.10 Ma) and isochron (red curve; 1.42 ± 0.28 Ma) modelling outputs, denoting three corresponding interglacial periods (cyan bands), MIS 47, 45 and 43. **b,** Isochron plot (red line $\pm 1\sigma$) fitted to $^{26}\text{Al}/^{10}\text{Be}$ data (plus signs with ellipses indicating $\pm 1\sigma$), showing the

post-burial $^{26}\text{Al}/^{10}\text{Be}$ production ratio (dashed black line). **c,** Hominin habitat suitability (blue line) for *H. erectus* (Mahalanobis erectus niche) generated for Korolevo (48°N , 23°E), 1.6–1.1 Ma (climate data server at <https://climatedata.ibs.re.kr>), with cosmogenic nuclide burial ages (top) and interglacials (pale blue bands) of potential hominin occupation. MIS boundaries are based on ref. 31.

suitability at Korolevo, in contrast to the relatively hostile conditions of the intervening glacial (Fig. 4c). This supports the idea that early hominins exploited warm interglacial periods to disperse into higher latitudes. Whether these early climate-mediated forays were episodic or semi-permanent will be determined only with additional securely dated sites. The advent of improved chronometry coupled with reconstructions of habitat is a major step forward for understanding the drivers of human migration.

Online content

Any methods, additional references, Nature Portfolio reporting summaries, source data, extended data, supplementary information, acknowledgements, peer review information; details of author contributions and competing interests; and statements of data and code availability are available at <https://doi.org/10.1038/s41586-024-07151-3>.

- Gladilin, V. N. The Korolevo Palaeolithic site: research methods, stratigraphy. *Anthropologie* **27**, 93–103 (1989).
- Adamenko, O. M. & Gladilin, V. N. Korolevo un des plus anciens habitats acheuléens et moustériens de Transcarpatie soviétique. *L'Anthropologie* **93**, 689–712 (1989).
- Koulakovska, L. V., Usik, V. & Haesaerts, P. Early Palaeolithic of Korolevo site (Transcarpathia, Ukraine). *Quat. Int.* **223–224**, 116–130 (2010).
- Balco, G. & Rovey, C. W. An isochron method for cosmogenic nuclide dating of buried soils and sediments. *Am. J. Sci.* **308**, 1083–1114 (2008).
- Knudsen, M. F. et al. New cosmogenic nuclide burial-dating model indicates onset of major glaciations in the Alps during Middle Pleistocene Transition. *Earth Planet. Sci. Lett.* **549**, 116491 (2020).
- Ferring, R. et al. Earliest human occupations at Dmanisi (Georgian Caucasus) dated to 1.85–1.78 Ma. *Proc. Natl Acad. Sci. USA* **108**, 10432–10436 (2011).
- Carbonell, E. et al. The first hominin of Europe. *Nature* **452**, 465–469 (2008).
- Michel, V. et al. New dating evidence of the early presence of hominins in Southern Europe. *Sci. Rep.* **7**, 10074 (2017).
- Timmermann, A. et al. Climate effects on archaic human habitats and species successions. *Nature* **604**, 495–501 (2022).
- Parés, J. M., Duval, M. & Arnold, L. J. New views on an old move: hominin migration into Eurasia. *Quat. Int.* **295**, 5–12 (2013).
- Muttoni, G., Scardia, G. & Kent, D. V. Early hominins in Europe: the Galerian migration hypothesis. *Quat. Sci. Rev.* **180**, 1–29 (2018).
- Falguères, C. The first human settlements out Africa into Europe: a chronological perspective. *Quat. Sci. Rev.* **247**, 106551 (2020).
- Channell, J. E. T., Singer, B. S. & Jicha, B. R. Timing of Quaternary geomagnetic reversals and excursions in volcanic and sedimentary archives. *Quat. Sci. Rev.* **228**, 106114 (2020).
- Muttoni, G., Scardia, G., Kent, D. V. & Martin, R. A. Bottleneck at Jaramillo for human migration to Iberia and the rest of Europe? *J. Hum. Evol.* **80**, 187–190 (2015).
- Gabunia, L. et al. Earliest Pleistocene hominid cranial remains from Dmanisi, republic of Georgia: taxonomy, geological setting, and age. *Science* **288**, 1019–1025 (2000).
- Garcia, T. et al. Earliest human remains in Eurasia: new $^{40}\text{Ar}/^{39}\text{Ar}$ dating of the Dmanisi hominid-bearing levels, Georgia. *Quat. Geochronol.* **5**, 443–451 (2010).
- Scardia, G. et al. Chronologic constraints on hominin dispersal outside Africa since 2.48 Ma from the Zarqa Valley, Jordan. *Quat. Sci. Rev.* **219**, 1–19 (2019).
- Lebatard, A. E. et al. Dating the *Homo erectus* bearing travertine from Kocabas (Denizli, Turkey) at least 1.1 Ma. *Earth Planet. Sci. Lett.* **390**, 8–18 (2014).
- Adamenko, O. M. et al. Paleolithic site of Korolevo in Transcarpathia. *Bull. Commiss. Invest. Quat. Period* **58**, 5–25 (1989). (in Russian).
- Usyk, V. I., Gerasimenko, N., Garba, R., Dambon, F. & Nigst, P. R. Exploring the potential of the Middle and Upper Palaeolithic Site Korolevo II (Ukraine): new results on stratigraphy, chronology and archaeological sequence. *J. Paleo. Arch.* **6**, 16 (2023).
- Haesaerts, P. & Koulakovska, L. in *The European Middle Palaeolithic* (ed. Koulakovska, L.) 21–37 (Institute of Archaeology, National Academy of Sciences, Ukraine, 2006).
- Nawrocki, J., Lanczont, M., Rosowiecka, O. & Bogucki, A. Magnetostratigraphy of the loess-palaeosol key Palaeolithic section at Korolevo (Transcarpathia, W Ukraine). *Quat. Int.* **399**, 72–85 (2016).
- Adamenko, O. et al. Reference magnetostratigraphic sections of anthropogenic deposits of Transcarpathia [in Russian]. *Proceedings of the Academy of Sciences of the USSR. Geological Series* **11**, 55–73 (1981).
- Rocca, R. First settlements in Central Europe: between originality and banality. *Quat. Int.* **409**, 213–221 (2016).
- Szymanek, M. & Julien, M. A. Early and Middle Pleistocene climate-environment conditions in Central Europe and the hominin settlement record. *Quat. Sci. Rev.* **198**, 56–75 (2018).
- Rácz, B., Szakmány, G. & Biró, K. T. Contribution to the cognizance of raw materials and raw material regions of the Transcarpathian Palaeolithic. *Acta Arch. Acad. Sci. Hungaricae* **67**, 209–229 (2016).
- Kamenik, J. et al. Processing of Korolevo samples aimed at AMS determination of in situ ^{10}Be and ^{26}Al nuclides and their purity control using follow-up mass spectrometry scans. *J. Radioanal. Nucl. Chem.* **332**, 1583–1590 (2023).
- Nørgaard, J., Jansen, J. D., Neuhuber, S., Ruszkiczay-Rüdiger, Z. & Knudsen, M. F. P-PINI: a cosmogenic nuclide burial dating method for landscapes undergoing non-steady erosion. *Quat. Geochronol.* **74**, 101420 (2023).
- Granger, D. E. in *Treatise on Geochemistry* 2nd edn (eds Holland, H. D. & Turekian, K. K.) 81–97 (Elsevier, 2014).
- Granger, D., Gibbon, R. & Kuman, K. New cosmogenic burial ages for Sterkfontein Member 2 Australopithecus and Member 5 Oldowan. *Nature* **522**, 85–88 (2015).
- Lisiecki, L. E. & Raymo, M. E. A Pliocene–Pleistocene stack of 57 globally distributed benthic $\delta^{18}\text{O}$ records. *Paleoceanography* **20**, PA1003 (2005).
- Leakey, M. D. *Olduvai Gorge: Excavations in Beds I & II 1960–1963* Vol. 3 (Cambridge Univ. Press, 1971).

33. Mgeladze, A. et al. Hominin occupations at the Dmanisi site, Georgia, Southern Caucasus: raw materials and technical behaviours of Europe's first hominins. *J. Hum. Evol.* **60**, 571–596 (2011).
34. Toro-Moyano, I. et al. The oldest human fossil in Europe, from Orce (Spain). *J. Hum. Evol.* **65**, 1–9 (2013).
35. Arzarello, M. et al. L'industrie lithique du site Pleistocene inferieur de Pirro Nord (Apricena, Italie du sud): une occupation humaine entre 1.3 et 1.7 Ma. *Anthropologie* **113**, 47–58 (2009).
36. Arzarello, M., De Weyer, L. & Peretto, C. The first European peopling and the Italian case: peculiarities and “opportunism”. *Quat. Int.* **393**, 41–50 (2016).
37. Chu, W. The Danube corridor hypothesis and the Carpathian Basin: geological, environmental and archaeological approaches to characterizing Aurignacian dynamics. *J. World Prehist.* **31**, 117–178 (2018).
38. Mellars, P. The earliest modern humans in Europe. *Nature* **479**, 483–485 (2011).
39. Sirakov, N. et al. An ancient continuous human presence in the Balkans and the beginnings of human settlements in western Eurasia: a lower Pleistocene example of the Lower Palaeolithic levels in Kozarnika cave (North-western Bulgaria). *Quat. Int.* **223–224**, 94–106 (2010).
40. Amirkhanov, H. A., Ozherelyev, D. V., Sablin, M. V. & Agadzhanian, A. K. Faunal remains from the Oldowan site of Mukhai II in the North Caucasus: potential for dating and paleolandscape reconstruction. *Quat. Int.* **395**, 233–241 (2016).
41. Shchenlinsky, V. E. et al. The Early Pleistocene site of Kermek in western Ciscaucasia (southern Russia): stratigraphy, biotic record and lithic industry (preliminary results). *Quat. Int.* **393**, 51–69 (2016).
42. Alvarez, C. et al. New magnetostratigraphic and numerical age of the Fuente Nueva-3 site (Guadix-Baza basin, Spain). *Quat. Int.* **389**, 224–234 (2015).
43. Bourguignon, L. et al. Bois-de-Riquet (Lézignan-la-Cèbe, Hérault): a late Early Pleistocene archaeological occurrence in southern France. *Quat. Int.* **393**, 24–40 (2016).
44. Antón, S. C. Natural history of *Homo erectus*. *Am. J. Phys. Anthropol.* **37**, 126–170 (2003).
45. Batchelor, C. L. et al. The configuration of Northern Hemisphere ice sheets through the Quaternary. *Nat. Commun.* **10**, 3713 (2019).
46. Chmeleff, J., von Blanckenburg, F., Kossert, K. & Jakob, D. Determination of the ¹⁰Be half-life by multicollector ICP-MS and liquid scintillation counting. *Nucl. Instr. Methods B* **268**, 192–199 (2010).
47. Korschinek, G. et al. A new value for the half-life of ¹⁰Be by heavy-ion elastic recoil detection and liquid scintillation counting. *Nucl. Instr. Methods B* **268**, 187–191 (2010).
48. Nishiizumi, K. Preparation of ²⁶Al AMS standards. *Nucl. Instr. Methods B* **223–224**, 388–392 (2004).
49. Akhmadaliev, S., Heller, R., Hanf, D., Rugel, G. & Merchel, S. The new 6MV AMS-facility DREAMS at Dresden. *Nucl. Instr. Methods B* **294**, 5–10 (2013).
50. Rugel, G. et al. The first four years of the AMS-facility DREAMS: status and developments for more accurate radionuclide data. *Nucl. Instr. Methods B* **370**, 94–100 (2016).

Publisher's note Springer Nature remains neutral with regard to jurisdictional claims in published maps and institutional affiliations.

Springer Nature or its licensor (e.g. a society or other partner) holds exclusive rights to this article under a publishing agreement with the author(s) or other rightsholder(s); author self-archiving of the accepted manuscript version of this article is solely governed by the terms of such publishing agreement and applicable law.

© The Author(s), under exclusive licence to Springer Nature Limited 2024

Methods

Burial dating with cosmogenic nuclides

When galactic cosmic radiation from outside the Solar System impinges on Earth's atmosphere, the high-energy particles (mostly protons) trigger cascades of secondary cosmic rays that induce nuclear reactions in soils and rocks at rates attenuating with depth below the ground surface⁵¹. Interactions with quartz grains produce rare radionuclides, such as ¹⁰Be and ²⁶Al, which can serve as a versatile chronometer capable of resolving the age of buried, quartz-bearing deposits back to 5 Ma (ref. 52).

Burial dating comes in three main variations. Simple burial dating tracks the decline in the ²⁶Al/¹⁰Be ratio for a single buried sample, assuming that burial is sufficiently rapid and deep to rule out post-burial nuclide production⁵². Isochron burial dating^{4,53} takes account of the ²⁶Al/¹⁰Be ratio measured in a suite of samples collected from a single stratigraphic unit. Both the simple and the isochron burial-dating methods assume that samples have experienced steady erosion in the sediment source area and continuous cosmic-ray exposure at the surface before their permanent burial. A third burial-dating method, P-PINI^{5,28}, is designed for settings characterized by abrupt, non-steady erosion, discontinuous exposure and elevation-dependent ²⁶Al/¹⁰Be production ratios in the source area⁵⁴, as well as changing depth in the burial zone through sediment accumulation or erosion over time. For Korolevo level VII, this means that P-PINI can readily simulate the slow accumulation of overlying loess, which is important for correctly estimating the post-burial nuclide production. P-PINI is an inversion model that merges a Monte Carlo simulator with the established cosmogenic nuclide production equations applied to a source-to-sink spatial framework^{5,28,55}. Millions of ¹⁰Be–²⁶Al inventories (or samples) are simulated (forward-modelled) in accordance with parameters chosen to track the accumulation, loss and decay of cosmogenic nuclides in the sediment source zone and depositional sink (that is, field sample site). The P-PINI set-up is designed so that all samples experience the same post-depositional accumulation rate preceded by differing pre-burial histories (from sample-specific source elevations). For Korolevo level VII, this means that each P-PINI simulation applies one post-burial accumulation rate and seven pre-burial erosion histories, and that the simulation is accepted only if it produces a good match for all seven samples (¹⁰Be–²⁶Al pairs). The most probable burial age is then calculated from all of the accepted simulations (see Supplementary Information for modelling details).

Here we apply both the P-PINI and the isochron burial methods to date level VII, the lowermost lithic assemblage at Korolevo I (Fig. 3). We then use P-PINI to recast the simple burial dating reported previously from Sima del Elefante, Atapuerca⁷. For all computations, we implement consistent parameter settings, including a range in the ²⁶Al/¹⁰Be surface production ratio of 6.75 to 7.15 (Supplementary Information).

Sampling and lab procedures

We measured cosmogenic ²⁶Al and ¹⁰Be in seven cobble-sized clasts collected from level VII (Fig. 2) during the 1985 Transcarpathian Palaeolithic Expedition and archived in the museum of the Institute of Archaeology, National Academy of Sciences of Ukraine (Supplementary Table 2 and Supplementary Fig. 4). Each of the seven clasts constitutes a single sample comprising vein quartz, quartzite or fine-grained sandstone. Initial preparation of physical samples was done at the Czech Geological Survey, followed by quartz purification, Be–Al extraction and accelerator mass spectrometry (AMS) measurement at the

Helmholtz-Zentrum Dresden-Rossendorf (DREAMS) using standard procedures^{50,56–59} (Supplementary Information). Additional quality control was applied during the sample preparation and AMS analysis²⁷.

Reporting summary

Further information on research design is available in the Nature Portfolio Reporting Summary linked to this article.

Data availability

All cosmogenic nuclide data used in this study are provided in Supplementary Table 3. Parameters used in our P-PINI model runs are given in Supplementary Tables 5–8. Parameters used in isochron burial dating are provided in Supplementary Table 4. The calculated hominin habitat suitability data are available on the climate data server at <https://climatedata.ibs.re.kr> linked to a previous study⁹.

Code availability

The MATLAB code used to generate burial ages with P-PINI (as shown in Fig. 4 and Supplementary Figs. 7–11) is shared at <https://github.com/CosmoAarhus/Korolevo>.

51. Gosse, J. C. & Phillips, F. M. Terrestrial in situ cosmogenic nuclides: theory and application. *Quat. Sci. Rev.* **20**, 1475–1560 (2001).
52. Granger, D. E. & Muzikar, P. F. Dating sediment burial with in situ-produced cosmogenic nuclides: theory, techniques, and limitations. *Earth Planet. Sci. Lett.* **188**, 269–281 (2001).
53. Erlanger, E., Granger, D. E. & Gibbon, R. J. Rock uplift rates in South Africa from isochron burial dating of fluvial and marine terraces. *Geology* **40**, 1019–1022 (2012).
54. Stone, J. O. Air pressure and cosmogenic isotope production. *J. Geophys. Res.* **105**, 23753–23759 (2000).
55. Balco, G. Production rate calculations for cosmic-ray-muon-produced ¹⁰Be and ²⁶Al benchmarked against geological calibration data. *Quat. Geochronol.* **39**, 150–173 (2017).
56. Merchel, S. & Herpers, U. An update on radiochemical separation techniques for the determination of long-lived radionuclides via accelerator mass spectrometry. *Radiochim. Acta* **84**, 215–220 (1999).
57. Merchel, S. et al. Towards more precise ¹⁰Be and ³⁶Cl data from measurements at the 10⁻¹⁴ level: influence of sample preparation. *Nucl. Instr. Methods B* **266**, 4921–4926 (2008).
58. Merchel, S. et al. Attempts to understand potential deficiencies in chemical procedures for AMS: cleaning and dissolving quartz for ¹⁰Be and ²⁶Al analysis. *Nucl. Instr. Methods B* **455**, 293–299 (2019).
59. Lachner, J. et al. Optimization of ¹⁰Be measurements at the 6 MV AMS facility DREAMS. *Nucl. Instr. Methods B* **535**, 29–33 (2023).

Acknowledgements We thank the DREAMS team at the Ion Beam Centre at the Helmholtz-Zentrum Dresden-Rossendorf for assistance with accelerator mass spectrometry; D. Granger and W. Odom for providing the MATLAB code describing the isochron model; and T. Fujioka for discussions about the Atapuerca sites. We acknowledge the following funding: Czech Ministry of Education, Youth and Sports (MEYS) (CZ.02.1.01/0.0/0.0/16_019/0000728); RADIATE (Horizon 2020, 824096) transnational access (21002366-ST); RADIATE guest researcher programme; MEYS (LM2018120); Czech Science Foundation (22-13190S); and Charles University Grant Agency (310222).

Author contributions Conceptualization: R.G., V.U. and J.D.J. Methodology: J.D.J., K.S., J. Kamenik, R.G., M.F.K., J.L., G.R., J. Kučera and F.V. Investigation: R.G., J. Kamenik, K.S., F.V., V.U., L.Y.-M., G.R., J.L., J.D.J. and M.F.K. Funding acquisition: R.G., J. Kamenik and J. Kučera. Project administration: R.G. Supervision: J.D.J. and J. Kučera. Writing (original draft): R.G., J.D.J., M.F.K., V.U., N.G. and A.I.R.H. Writing (review and editing): J.D.J., M.F.K., R.G., N.G., A.I.R.H., V.U., J. Kamenik, J. Kučera, K.S., J.L., G.R. and F.V.

Competing interests The authors declare no competing interests.

Additional information

Supplementary information The online version contains supplementary material available at <https://doi.org/10.1038/s41586-024-07151-3>.

Correspondence and requests for materials should be addressed to R. Garba, M. F. Knudsen or J. D. Jansen.

Peer review information Nature thanks Darryl Granger and the other, anonymous, reviewer(s) for their contribution to the peer review of this work.

Reprints and permissions information is available at <http://www.nature.com/reprints>.

Reporting Summary

Nature Portfolio wishes to improve the reproducibility of the work that we publish. This form provides structure for consistency and transparency in reporting. For further information on Nature Portfolio policies, see our [Editorial Policies](#) and the [Editorial Policy Checklist](#).

Statistics

For all statistical analyses, confirm that the following items are present in the figure legend, table legend, main text, or Methods section.

n/a	Confirmed
<input type="checkbox"/>	<input checked="" type="checkbox"/> The exact sample size (n) for each experimental group/condition, given as a discrete number and unit of measurement
<input checked="" type="checkbox"/>	<input type="checkbox"/> A statement on whether measurements were taken from distinct samples or whether the same sample was measured repeatedly
<input checked="" type="checkbox"/>	<input type="checkbox"/> The statistical test(s) used AND whether they are one- or two-sided <i>Only common tests should be described solely by name; describe more complex techniques in the Methods section.</i>
<input checked="" type="checkbox"/>	<input type="checkbox"/> A description of all covariates tested
<input checked="" type="checkbox"/>	<input type="checkbox"/> A description of any assumptions or corrections, such as tests of normality and adjustment for multiple comparisons
<input type="checkbox"/>	<input checked="" type="checkbox"/> A full description of the statistical parameters including central tendency (e.g. means) or other basic estimates (e.g. regression coefficient) AND variation (e.g. standard deviation) or associated estimates of uncertainty (e.g. confidence intervals)
<input checked="" type="checkbox"/>	<input type="checkbox"/> For null hypothesis testing, the test statistic (e.g. F , t , r) with confidence intervals, effect sizes, degrees of freedom and P value noted <i>Give P values as exact values whenever suitable.</i>
<input type="checkbox"/>	<input checked="" type="checkbox"/> For Bayesian analysis, information on the choice of priors and Markov chain Monte Carlo settings
<input checked="" type="checkbox"/>	<input type="checkbox"/> For hierarchical and complex designs, identification of the appropriate level for tests and full reporting of outcomes
<input checked="" type="checkbox"/>	<input type="checkbox"/> Estimates of effect sizes (e.g. Cohen's d , Pearson's r), indicating how they were calculated

Our web collection on [statistics for biologists](#) contains articles on many of the points above.

Software and code

Policy information about [availability of computer code](#)

Data collection	A custom operational software of Accelerator Mass Spectrometry instrument at Institute of Ion Beam Physics and Materials Research, Helmholtz-Zentrum Dresden Rossendorf was used for analysis of ^{10}Be and ^{26}Al concentrations.
Data analysis	The Isochron and P-PINI codes were used in software MATLAB R2021b. The MATLAB code used to generate the P-PINI burial ages is shared on https://github.com/CosmoAarhus/Korolevo . P-PINI version 1.02 was used.

For manuscripts utilizing custom algorithms or software that are central to the research but not yet described in published literature, software must be made available to editors and reviewers. We strongly encourage code deposition in a community repository (e.g. GitHub). See the Nature Portfolio [guidelines for submitting code & software](#) for further information.

Data

Policy information about [availability of data](#)

All manuscripts must include a [data availability statement](#). This statement should provide the following information, where applicable:

- Accession codes, unique identifiers, or web links for publicly available datasets
- A description of any restrictions on data availability
- For clinical datasets or third party data, please ensure that the statement adheres to our [policy](#)

Accelerator mass spectrometry analysis of ^{10}Be and ^{26}Al concentrations are provided in Table 1. and in extended form in Supplementary Table S3. The P-PINI parameters are provided in Supplementary Tables S5–S8. Parameters used in isochron burial dating are provided in Table S4. There are no restriction on data usage

and access. The calculated hominin habitat suitability data are available on the climate data server at <https://climatedata.ibs.re.kr> linked to Timmerman et al. (2022) doi: 10.1038/s41586-022-04600-9. The map on Fig. 1 was generated using QGIS version 3.26.3-Buenos Aires, map GeoTIFF data source, GEBCO Compilation Group (2022) The GEBCO 2022 Grid (<http://gebco.net>), geo. projection EPSG:3035 was used.

Research involving human participants, their data, or biological material

Policy information about studies with [human participants or human data](#). See also policy information about [sex, gender \(identity/presentation\), and sexual orientation](#) and [race, ethnicity and racism](#).

Reporting on sex and gender	N/A
Reporting on race, ethnicity, or other socially relevant groupings	N/A
Population characteristics	N/A
Recruitment	N/A
Ethics oversight	N/A

Note that full information on the approval of the study protocol must also be provided in the manuscript.

Field-specific reporting

Please select the one below that is the best fit for your research. If you are not sure, read the appropriate sections before making your selection.

Life sciences Behavioural & social sciences Ecological, evolutionary & environmental sciences

For a reference copy of the document with all sections, see nature.com/documents/nr-reporting-summary-flat.pdf

Ecological, evolutionary & environmental sciences study design

All studies must disclose on these points even when the disclosure is negative.

Study description	An assemblage of stone tools stratified in alluvium and loess at Korolevo, western Ukraine, has been studied by multiple research groups since the site's discovery in the 1970s. Despite wide acknowledgement of Korolevo's importance to the European Early Paleolithic, age constraints on the lowermost lithic artifacts in cultural level VII have remained inconclusive. The ^{26}Al - ^{10}Be cosmogenic nuclide inventory of seven gravel clasts from the lowermost cultural layer (level VII) was measured to constrain the age of the first hominin presence at Korolevo using P-PINI (Particle Pathway Inversion of Nuclide Inventories) and isochron burial dating methods.
Research sample	Seven cobble-sized samples from the lowermost cultural layer VII of different lithology (vein quartz, quartzite, fine-grained sandstone) and mass were selected from the collection of the Transcarpathian Palaeolithic Expedition 1984-1985 from the Archaeological Museum of the Institute of Archaeology in Kyiv. The sample qualification process with sample exclusions prior to Accelerator Mass Spectrometry (AMS) analysis is described in Supplementary Table S2.
Sampling strategy	The sampling strategy was designed from the outset to use isochron and P-PINI advanced cosmogenic nuclide burial age dating methods, which use multiple samples from the same strata to calculate burial age. In contrast to simple single-sample burial age, the use of seven samples in the burial age isochron model can remove most of the uncertainties associated with post-burial production. The use of P-PINI (Particle Pathway Inversion of Nuclide Inventories) is a newly developed dating tool that uses inverse Monte Carlo modelling of cosmogenic nuclide abundances to estimate the burial age and history of sedimentary deposits. While the isochron and P-PINI methods yield overlapping ages, we favour the P-PINI result because it readily accounts for (1) non-steady erosion in the catchment prior to sediment burial, (2) catchments with elevation-dependent $^{26}\text{Al}/^{10}\text{Be}$ ratios, (3) sample-specific source elevations, and (4) the slow accumulation of loess units in the profile over time (Fig. 2). Moreover, P-PINI delivers a far tighter uncertainty range.
Data collection	The initial physical quartz cleaning and inspection was carried out at the Czech Geological Survey, the final physical and chemical cleaning, including the preparation of pure BeO and Al_2O_3 for AMS measurements of ^{10}Be and ^{26}Al concentrations, was carried out at the Dresden Accelerator Mass Spectrometry (DREAMS) facility at the Helmholtz-Zentrum Dresden-Rossendorf (HZDR). The AMS measurements of the Be and Al isotope ratios were performed at HZDR using the DREAMS accelerator mass spectrometer.
Timing and spatial scale	Physical sample preparation (Aug-Oct 2021) Chemical sample treatment and oxide preparation (Nov-Dec 2021 & Mar 2022) AMS beamtime and analysis (Mar 2022 for Be; May 2022 for Al)
Data exclusions	Sample KOR-ISO-7B was not included, sample suspected of insufficient quartz purification (Supp. Mat.).
Reproducibility	Our study is based on discrete physical samples (rock clasts) from the 1984-1985 archaeological excavations. The burial age calculations are highly reproducible using other computer platforms or other calculation methods.

Randomization The P-PINI-derived ^{10}Be - ^{26}Al 'library' comprises 10 million virtual samples simulated for the Korolevo samples. Supplementary Figure S7 shows seven Korolevo samples together with the simulations accepted as having comparable inventories with the uncertainty of the corresponding samples.

Blinding Blinding is not applicable to our numerical model simulations, as the same code will generate the same simulation employing other computer platform, which use the same numerical precision.

Did the study involve field work? Yes No

Field work, collection and transport

Field conditions Between 1974 and 2017, more than 50 sondages, excavations and profiles were carried out in the area of three archaeological sites (Supplementary Fig. S1): Korolevo I - Gostry Verkh, Korolevo I - Beyvar, and Korolevo II. In 1984-85, sondages 14, 18, 26 and excavations XII, X/XIII of the 12 m loess-palaeosol sequence were conducted at Gostry verkh for archaeological, micromorphological, palaeopedological, palynological, litho-mineralogical, palaeomagnetic, thermoluminescence, palaeomagnetic, and radiocarbon dating studies together with study of lithic artefacts.

Location Korolevo site (Gostry Verkh) 23.167 E 48.176 N

Access & import/export The pebble samples were collected during the excavations of the Transcarpathian Palaeolithic Expedition in 1985. Authors Usyk and Gerasimenko actively participated in most of the field campaigns at Korolevo. Authors Garba and Usyk visited the site in the summer of 2021 and August 2023 to assess the state of conservation of the site and to discuss steps for its protection. The formal agreement for sample exchange, collection and revision of the chronostratigraphic model of the Korolevo site using cosmogenic nuclide dating was signed in 2021 between the Institute of Nuclear Physics of the Czech Academy of Sciences and the Institute of Archaeology of the Ukrainian Academy of Sciences.

Disturbance The study involved no direct disturbance to the site itself, as the samples were provided from the existing collection of the 1984-1985 Transcarpathian Palaeolithic Expedition at the Archaeological Museum of the Institute of Archaeology in Kyiv.

Reporting for specific materials, systems and methods

We require information from authors about some types of materials, experimental systems and methods used in many studies. Here, indicate whether each material, system or method listed is relevant to your study. If you are not sure if a list item applies to your research, read the appropriate section before selecting a response.

Materials & experimental systems

n/a	Involvement
<input checked="" type="checkbox"/>	<input type="checkbox"/> Antibodies
<input checked="" type="checkbox"/>	<input type="checkbox"/> Eukaryotic cell lines
<input checked="" type="checkbox"/>	<input type="checkbox"/> Palaeontology and archaeology
<input checked="" type="checkbox"/>	<input type="checkbox"/> Animals and other organisms
<input checked="" type="checkbox"/>	<input type="checkbox"/> Clinical data
<input checked="" type="checkbox"/>	<input type="checkbox"/> Dual use research of concern
<input checked="" type="checkbox"/>	<input type="checkbox"/> Plants

Methods

n/a	Involvement
<input checked="" type="checkbox"/>	<input type="checkbox"/> ChIP-seq
<input checked="" type="checkbox"/>	<input type="checkbox"/> Flow cytometry
<input checked="" type="checkbox"/>	<input type="checkbox"/> MRI-based neuroimaging